CrystEngComm

RSC Publishing

PAPER

View Article Online
View Journal | View Issue

Cite this: *CrystEngComm*, 2013, **15**, 10533

Preparation of water-dispersible TiO_2 nanoparticles from titanium tetrachloride using urea hydrogen peroxide as an oxygen donor†

Naoko Watanabe,[a] Taichi Kaneko,[a] Yuko Uchimaru,[b] Sayaka Yanagida,[c] Atsuo Yasumori[c] and Yoshiyuki Sugahara*[ad]

Received 6th August 2013,
Accepted 30th September 2013

DOI: 10.1039/c3ce41561a

www.rsc.org/crystengcomm

TiO_2 nanoparticles were prepared from titanium tetrachloride ($TiCl_4$) in CH_2Cl_2 at 80 °C for 30 h, 42 h and 70 h using urea hydrogen peroxide (UHP) as an oxygen donor with a $TiCl_4$: UHP molar ratio of 1 : 2. The XRD patterns and Raman spectroscopy results showed that the products consisted of anatase TiO_2. IR and solid-state ^{13}C NMR with cross polarization and magic angle spinning techniques revealed the presence of urea. TEM observation revealed that the products prepared by the reactions for 30 and 42 h consisted of water-dispersible spheroid nanoparticles with a long axis of ~5 nm, while an aggregation of nanoparticles was evident upon reaction for 70 h. Thermogravimetry, inductively-coupled plasma emission spectrometry and CHN analysis showed that the amount of urea increases in the following order: TiO_2_42h, TiO_2_70h, TiO_2_30h. The photocatalytic activity of the products dispersible in water (TiO_2_30h and TiO_2_42h) was estimated based on the degradation behaviour of methylene blue, and TiO_2_42h showed higher photocatalytic activity than TiO_2_30h. It is proposed that $TiCl_4$ was directly oxidized by UHP to form anatase TiO_2 in the early stage of the process.

Introduction

Nanochemistry has been developed for the preparation of nanostructures, which are of particular interest because of their interesting chemical, physical and biological behaviour.[1] Among nanostructures, nanoparticles (NPs) are attracting considerable attention since they can exhibit properties superior to those of large particles based on their large surface areas and quantum effect.[2] So far, a variety of applications have been developed using many kinds of NPs.[3] Titania (TiO_2) is an attractive functional oxide since it exhibits interesting photochemical and optical properties, including photocatalytic activity and high refractive indices.[4,5] The preparation of TiO_2 NPs has consequently been achieved with many different techniques, such as hydrolytic sol–gel, hydrothermal/solvothermal synthesis, and electrochemical deposition.[6–8]

Among the various preparation techniques for TiO_2 NPs, a non-hydrolytic sol–gel process has been employed for the preparation of TiO_2 NPs.[9–12] Titanium tetrahalides, typically titanium tetrachloride ($TiCl_4$), have been utilized in this process. $TiCl_4$ was reacted with an oxygen donor, such as diisporopylether, or a titanium alkoxide, typically titanium tetraisopropoxide.[13,14] Since these reactions were conducted in organic solvents without the presence of H_2O (which can also act as an oxygen donor), one of the advantages of this non-hydrolytic sol–gel process is the ability to control the amount of oxygen in the entire process, and this kind of control is extremely attractive for the size control of TiO_2 NPs.[9,11]

Hydrogen peroxide (H_2O_2), another oxygen donor, has been utilized in the preparation of limited types of metal oxides, such as ZnO_2, Fe_2O_3 and Fe_3O_4.[15–18] H_2O_2 has also been utilized as a ligand in Ti complexes, and the resulting complexes can be water-soluble precursors for TiO_2.[19–23] H_2O_2 has also been utilized as an oxidizing reagent in organic synthesis.[24–26] H_2O_2 is available only as aqueous solutions, which limits its usage in organic synthesis to a large extent. Urea-hydrogen peroxide (UHP; $CO(NH_2)_2{\cdot}H_2O_2$) is a 1 : 1 adduct between urea and hydrogen peroxide.[27] It can be prepared easily from an aqueous solution of urea and H_2O_2, and it is also inexpensive and commercially available.[28,29] Since UHP is soluble in some organic solvents, such as

[a] *Department of Applied Chemistry, School of Advanced Science and Engineering, Waseda University, Ohkubo-3, Shinjuku-ku, Tokyo 169-8555, Japan. E-mail: ys6546@waseda.jp*
[b] *National Institute of Advanced Industrial Science and Technology (AIST), Central 5, Higashi, Tsukuba, Ibaraki 305-8565, Japan*
[c] *Department of Materials Science and Technology, Faculty of Industrial Science and Technology, Tokyo University of Science, Yamazaki-2641, Noda, Chiba 278-8510, Japan*
[d] *Kagami Memorial Laboratory for Materials Science and Technology, Waseda University, Nishiwaseda-2, Shinjuku-ku, Tokyo, 169-0051, Japan*
† Electronic supplementary information (ESI) available. See DOI: 10.1039/c3ce41561a

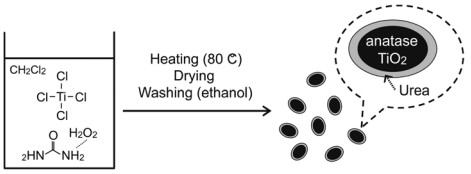

Fig. 1 Overview of the preparation of the water-dispersible anatase TiO_2 nanoparticles.

alcohols and chloroform,[29] UHP has been utilized for oxidation reactions such as epoxidation and sulfide oxidation.[29,30]

Here, we report the first application of UHP for metal oxide preparation. UHP can possibly play multiple roles, as an oxidation reagent as well as a donor of water which can cause hydrolysis, and urea which can coordinate to Lewis acid sites. In the present study, TiO_2 NPs have been prepared by a reaction of $TiCl_4$ with UHP in dichloromethane (CH_2Cl_2). The resulting products consist of water-dispersible TiO_2 spheroid NPs with a long axis of ~5 nm. An overview of the preparation of water-dispersible anatase TiO_2 NPs using UHP is illustrated in Fig. 1.

Experimental

General information

X-ray diffraction (XRD) patterns were obtained with a Rigaku RINT-2500 diffractometer (Ni-filtered CuK_α radiation). Raman spectra were obtained with a Renishaw in Via Reflex spectrometer using a 532 nm laser. Infrared (IR) spectra were recorded on a JASCO FT/IR-460 Plus spectrometer using the KBr method. Samples were dried under reduced pressure before preparing KBr disks. Solid-state ^{13}C nuclear magnetic resonance (NMR) spectroscopy was performed with a JEOL ECX-400 spectrometer at 99.55 MHz. Solid-state ^{13}C NMR spectra were obtained with cross-polarization (CP) and magic angle spinning (MAS) techniques (pulse delay, 10 s; contact time, 5 ms; spinning rate, 8 kHz). Transmission electron microscopy (TEM) images were obtained on a JEOL JEM-1011 microscope operating at 100 kV. TEM samples were prepared by evaporating a diluted aqueous dispersion of TiO_2 NPs on carbon supported on a copper mesh TEM grid. Field-emission transmission electron microscopy (FE-TEM) images were obtained with a Hitachi HF-2200 microscope operating at 100 kV. The Brunauer–Emmett–Teller (BET) specific surface areas of the products were determined by the N_2 adsorption–desorption method at −196 °C with a BELSORP-mini II instrument and preliminary drying at 150 °C for 1 h. Thermogravimetry (TG) was performed with a Rigaku TG8120 Thermoplus EVO thermobalance in the range of 50 to 1000 °C with a heating rate of 10 °C min^{-1} under a nitrogen flow. Inductively coupled plasma (ICP) emission spectrometry was performed with a Varian Vista-MPX CCD Simultaneous ICP-OES instrument after dissolving the products (1.2 mg) in 12 mL of a mixed solution (prepared from 80 mL of H_2SO_4 and 27 g of $SO_4(NH_4)_2$) at 150 °C. Elemental analysis (CHN) was performed with a Perkin Elmer PE2400II instrument. Ion chromatography (IC) was performed with a Japan Dionex ICS-90 instrument after dissolving 5 mg of the product in 0.2 mL of H_2SO_4 and subsequently diluting to 100 mL. Cl_2 gas was detected with Gastec Passive Dositube No. 8D. The average concentration of Cl_2 after 20 h was obtained by opening the autoclaves in a glovebag filled with nitrogen. Ultraviolet-visible (UV-Vis) spectra were obtained with Jasco V-630 and Shimadzu PC-2400 spectrometers.

Materials

The TiO_2 NPs were prepared using UHP (97%, H_2O_2 35%, Aldrich) as an oxygen donor, $TiCl_4$ (1.0 M, in dichloromethane) as the Ti source, and CH_2Cl_2 as a solvent. CH_2Cl_2 was distilled over CaH_2. Ethanol was used as a washing solvent without further purification. Urea, $CO(NH_2)_2$ (99.0%), and aqueous hydrogen peroxide, H_2O_2 (30.0%), were used in control experiments without further purification. Methylene blue was used for the measurements of the photocatalytic activity. Sulfuric acid (H_2SO_4, >96%) and $SO_4(NH_4)_2$ (99.5%) were used without further purification.

Preparation of the TiO_2 nanoparticles using UHP

All manipulations conducted before sealing the autoclave were carried out in a glovebox filled with nitrogen. The reaction was performed in a 20 mL Teflon-lined stainless autoclave. A CH_2Cl_2 solution of $TiCl_4$ (6.50 mL, corresponding to 6.50 mmol $TiCl_4$) was added to UHP (1.22 g, 13.0 mmol) in the autoclaves ($TiCl_4$: UHP molar ratio of 1 : 2). The autoclave was then sealed following the addition of CH_2Cl_2 (10.0 mL) to the mixture in the autoclave. The autoclave was heated in an oven at 80 °C for 20, 30, 42, and 70 h. The resultant white solids were centrifuged, washed twice with ethanol, and dried under reduced pressure at ambient temperature. The 70 h product was washed four times. The products were labelled TiO_2_*x*h, where *x* is the reaction period.

Photocatalytic activity of the TiO_2 nanoparticles dispersed in water

The photocatalytic activity of the products was evaluated by degrading methylene blue in an aqueous solution. TiO_2_30h or TiO_2_42h was dispersed in water (0.5 mass%) to obtain a highly transparent dispersion. The aqueous TiO_2 dispersion, methylene blue and deionized water were then mixed. The mixture contained 0.0100 mass% TiO_2 and 0.0100 mmol L^{-1} methylene blue. The mixture was transferred to a cylindrical glass beaker (inside diameter: 55.3 mm and height: 59.6 mm). Before the photocatalytic activity measurements, the aqueous TiO_2 dispersion was sonicated for 10 min. The aqueous TiO_2 dispersion was stirred continuously in an ice bath under a BLB lamp (FL15 BLB, TOSHIBA) (0.50 mW cm^{-2} at 365 nm). The maximum absorbance (664.5 nm) of methylene blue was measured after 15, 30, 45, 60, 90, 120, 150, and 180 min with a UV-Vis spectrometer.

Control experiments: preparation of the TiO_2 nanoparticles without using UHP

Control experiments were conducted without using UHP. All manipulations conducted before sealing the autoclave were carried out in a glovebag filled with nitrogen.

$TiCl_4$–H_2O_2/H_2O–urea–CH_2Cl_2 system (TiO_2_H_2O_2_urea): a CH_2Cl_2 solution of $TiCl_4$ CH_2Cl_2 (6.50 mL, corresponding to 6.50 mmol $TiCl_4$) was added to 30% aqueous H_2O_2 (1.47 mL, 13.0 mmol H_2O_2) and urea (0.781 g, 13.0 mmol) in an autoclave ($TiCl_4$: urea : H_2O_2 : water = 1 : 2 : 2 : 9 in a molar ratio). The autoclave was then sealed following the addition of CH_2Cl_2 (10.0 mL) to the mixture in the autoclave.

$TiCl_4$–H_2O–urea–CH_2Cl_2 system (TiO_2_water_urea): a CH_2Cl_2 solution of $TiCl_4$ (6.50 mL, corresponding to 6.50 mmol $TiCl_4$) was added to water (1.47 mL, 57.2 mmol) and urea (0.781 g, 13.0 mmol) in an autoclave ($TiCl_4$: urea : water = 1 : 2 : 13 in a molar ratio). The autoclave was then sealed following the addition of CH_2Cl_2 (10.0 mL) to the mixture in the autoclave.

$TiCl_4$–H_2O_2/H_2O–CH_2Cl_2 system (TiO_2_H_2O_2): a CH_2Cl_2 solution of $TiCl_4$ (6.50 mL, corresponding to 6.50 mmol $TiCl_4$) was added to 30% aqueous H_2O_2 (1.47 mL, 13.0 mmol H_2O_2) in an autoclave ($TiCl_4$: H_2O_2 : water = 1 : 2 : 9 in a molar ratio). The autoclave was then sealed following the addition of CH_2Cl_2 (10.0 mL) to the mixture in the autoclave.

These autoclaves were heated in an oven at 80 °C for 30 h. The resultant solids were centrifuged, washed twice with ethanol, and dried under reduced pressure at ambient temperature.

Results and discussion

Preparation of the TiO_2 nanoparticles using UHP

White smoke was formed when the autoclave used for the preparation of TiO_2_20h was opened, a result showing that $TiCl_4$ did not react completely and that a considerable number of Ti–Cl bonds remained upon reaction for 20 h. TiO_2_30h, TiO_2_42h and TiO_2_70h were obtained as mixtures of transparent liquids and white solids, on the other hand, and fine white powders were obtained after these products were washed and dried. Thus, the characterization results of TiO_2_30h, TiO_2_42h and TiO_2_70h are described hereafter. The Ti-based yields of TiO_2_30h, TiO_2_42h and TiO_2_70h were 77, 71, and 77%, respectively.

Fig. 2 shows the XRD patterns of the products. TiO_2_30h, TiO_2_42h and TiO_2_70h correspond to anatase TiO_2 (JCPDS no. 21-1272). It should be noted that the XRD profile does not change with variations in the reaction time. The XRD pattern of TiO_2_70h also showed the presence of NH_4Cl (JCPDS no. 7-8), however, when TiO_2_70h was washed twice with ethanol (Fig. S1, ESI†), and TiO_2_70h was thus washed four times. It should be noted that NH_4Cl was also detected in unwashed TiO_2_30h and TiO_2_42h. NH_4Cl seems to be formed from NH_3 and HCl because of the hydrolysis of urea and $TiCl_4$.[31,32] The crystallite size of TiO_2_30h, TiO_2_42h and TiO_2_70h calculated from the (101) reflections using

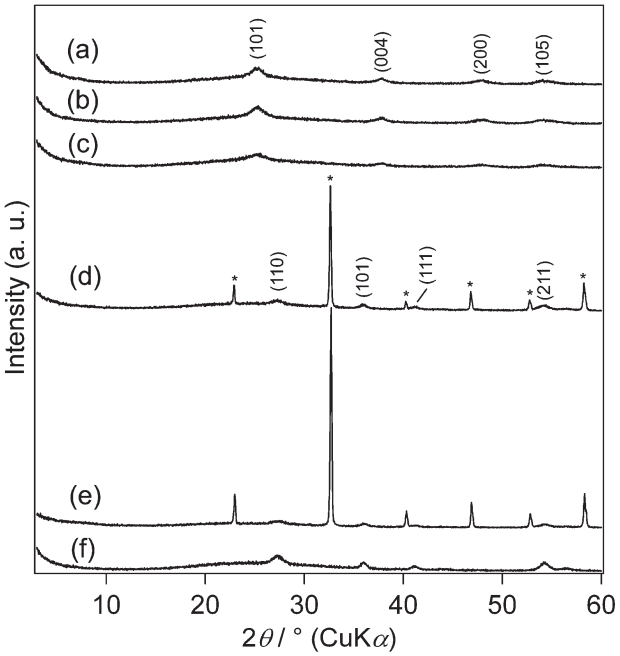

Fig. 2 XRD patterns of (a) TiO_2_30h, (b) TiO_2_42h, (c) TiO_2_70h, (d) TiO_2_H_2O_2_urea, (e) TiO_2_water_urea and (f) TiO_2_H_2O_2 (*: NH_4Cl).

Scherrer's formula[33] were 8.7, 8.9 and 8.3 nm, respectively. These results demonstrate that the crystalline phase and particle size of these products remained unchanged, regardless of the reaction time.

The products were further characterized by Raman spectroscopy (Fig. 3). The Raman spectrum of TiO_2_30h shows bands at 154.4, 398.9, 514.6 and 639.7 cm^{-1}. Bands at 153.1, 399.2, 513.4 and 640.0 cm^{-1} are present in the Raman

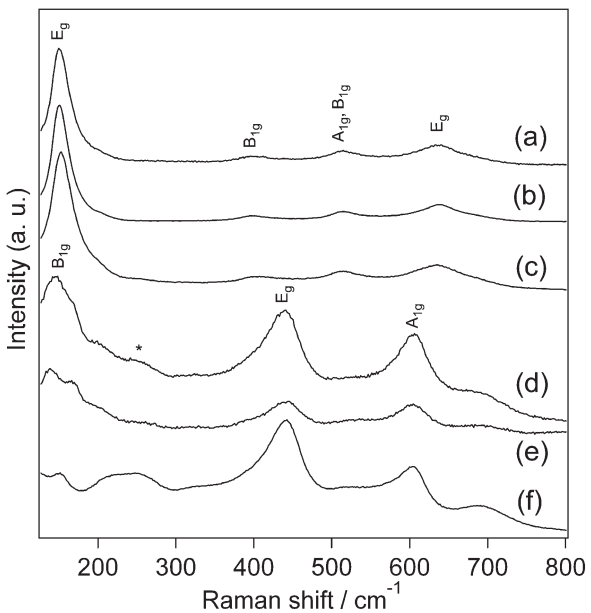

Fig. 3 Raman spectra of (a) TiO_2_30h, (b) TiO_2_42h, (c) TiO_2_70h, (d) TiO_2_H_2O_2_urea, (e) TiO_2_water_urea and (f) TiO_2_H_2O_2 (*: two phonon scattering).

spectrum of TiO_2_42h. The Raman spectrum of TiO_2_70h exhibits bands at 153.1, 399.2, 513.4 and 640.0 cm^{-1}. These bands are assignable to anatase TiO_2,[34] as shown in Fig. 3. Thus, the Raman results are in accordance with the XRD observations. It was reported that the Raman shifts of the strongest E_g band near 154 cm^{-1} was sensitive to the particle size of TiO_2 NPs, and the variations in the E_g band positions have been discussed in terms of phonon confinement,[34,35] oxygen deficiency,[36,37] and internal stress/surface tension effects.[38,39] Thus, the Raman results are consistent with the formation of anatase TiO_2 NPs.

Fig. 4 shows the IR spectra of the products and UHP. The O–O stretching band at 871 cm^{-1} [21] of UHP disappears in all the spectra of the products, indicating that UHP did not remain as a solid. Broad bands between 950–700 and 600–400 cm^{-1}, characteristic of the Ti–O stretching modes,[40] are present in the spectra of all the products, which is consistent with TiO_2 formation. In addition, bands assignable to urea are observed at ~3420 [br, $\nu_{as}(NH_2)$], ~3230 [br, $\nu_s(NH_2)$], 1640 [ν(CO), $\rho(NH_2)$], 1561–1562 (the assignment of this band will be discussed in the following paragraph), 1399–1401 [ν(CN)], and 1154–1156 [$\rho(NH_2)$] in the spectra of TiO_2_30h, TiO_2_42h and TiO_2_70h.[41] In addition, the ^{13}C CP/MAS NMR spectrum of TiO_2_30h exhibits a signal that is assignable to urea at 163 ppm[42] (Fig. S2, ESI†).

The adsorption of urea on anatase TiO_2 surfaces has been investigated using IR. It was reported that urea molecules adsorbed on anatase TiO_2 surfaces exhibited characteristic bands at 1562–1552 cm^{-1}, and based on the IR results, coordination of one of two nitrogen atoms in the urea molecule to the anatase TiO_2 surface was proposed.[43] IR spectra simulated for similar coordination arrangements as well as those of urea adsorbed on anatase TiO_2 surfaces *via* the vapour phase were reported, and similar bands were present.[44] Thus, the presence of the bands at 1561–1562 cm^{-1} strongly suggests a similar interaction between urea and the anatase TiO_2 surfaces in the present study, and the bands are accordingly assigned to the ν_{as}(Ti–OCN–Ti) mode.

MFurther structural characterization of the products was carried out using TEM and FE-TEM. Fig. 5 shows the TEM and FE-TEM images of TiO_2_30h, TiO_2_42h and TiO_2_70h. The TEM images of TiO_2_30h, TiO_2_42h and TiO_2_70h show aggregated spheroid TiO_2 NPs in aggregation sizes of about 10, 10–25 and 25–100 nm, respectively. In addition, the FE-TEM images of the products show the formation of spheroid NPs with a long axis of ~5 nm. This particle size is close to the crystallite size values estimated by Scherrer's formula. Thus, spheroid NPs with a long axis of ~5 nm tend to aggregate with an increase in reaction time. The lattice fringe, with a spacing of 0.35 nm, corresponds to the spacing of the (101) planes of anatase TiO_2. It was reported that amines acted as shape controllers to yield spheroid NPs by their specific adsorption to the crystal planes parallel to the *c*-axis of TiO_2 NPs.[45,46] Since the IR results suggest that the NH_2 groups of urea interacted with anatase TiO_2, spheroid NPs are also likely to be obtained in the present study because of urea adsorption on TiO_2 NPs.

The specific surface areas were estimated by the BET method (S_{BET}). Fig. S3 in the ESI† shows nitrogen adsorption–desorption isotherms of TiO_2_30h, TiO_2_42h, and TiO_2_70h. The S_{BET} values of TiO_2_30h, TiO_2_42h and TiO_2_70h were 231, 281, 247 $m^2\ g^{-1}$, respectively.

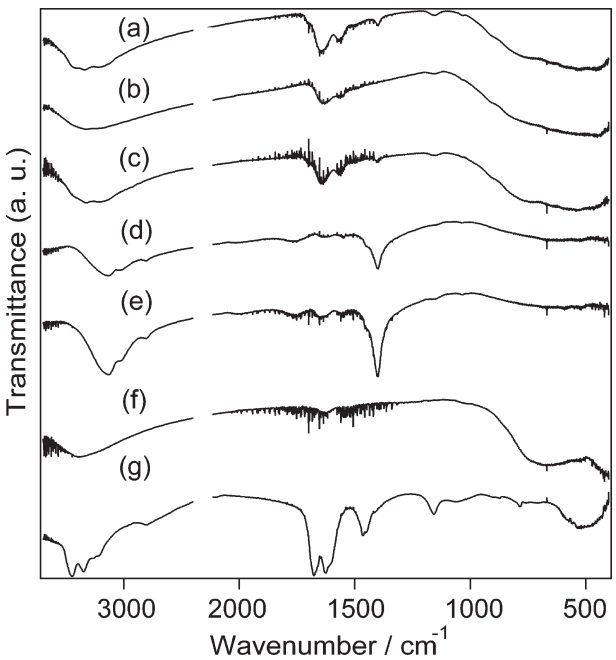

Fig. 4 IR spectra of (a) TiO_2_30h, (b) TiO_2_42h, (c) TiO_2_70h, (d) TiO_2_H_2O_2_urea, (e) TiO_2_water_urea, (f) TiO_2_H_2O_2 and (g) UHP.

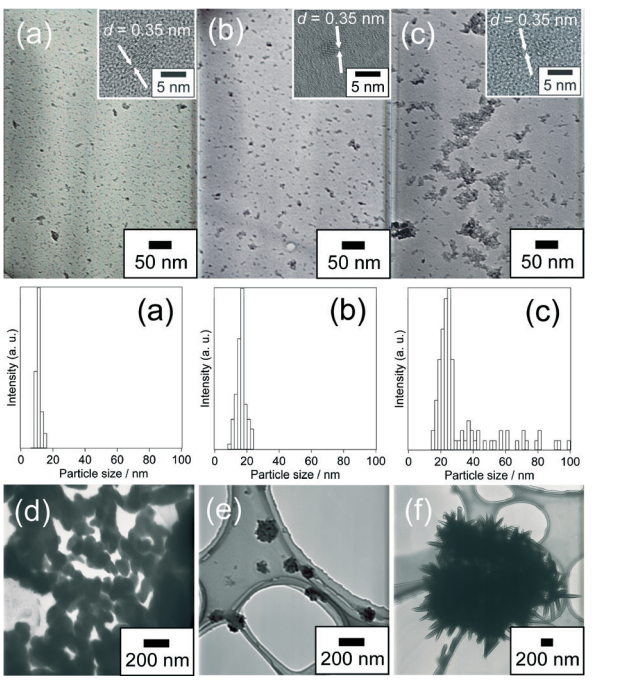

Fig. 5 TEM and FE-TEM images of (a) TiO_2_30h, (b) TiO_2_42h, (c) TiO_2_70h, (d) TiO_2_H_2O_2_urea, (e) TiO_2_water_urea, (f) TiO_2_H_2O_2 and size distributions are shown for (a)–(c).

Fig. S4 in the ESI† shows the TG curves of the products. The total mass losses up to 1000 °C of TiO_2_30h, TiO_2_42h and TiO_2_70h are 23.7, 17.0 and 18.9 mass%, respectively. The molar ratios of Ti and urea in the products were measured by ICP and CHN analyses. The amounts of urea per Ti in TiO_2_30h, TiO_2_42h and TiO_2_70h were 0.28, 0.12 and 0.17 (in mol), respectively (Table 1). The urea and adsorbed water ratios of the products were calculated based on the total mass loss of the TG curves and the molar ratios of Ti and urea. By assuming that all the organics are present as urea, the mass losses due to the thermal decomposition of urea in TiO_2_30h, TiO_2_42h and TiO_2_70h are estimated to be 15.5, 6.6 and 9.8 mass%, respectively. The mass losses due to the evaporation of adsorbed water in TiO_2_30h, TiO_2_42h and TiO_2_70h are calculated to be 8.0, 10.4 and 9.1 mass%, respectively (Table 1). Thus, the content of urea on the surface of the TiO_2 NPs is increasing in the following order: TiO_2_40h < TiO_2_70h < TiO_2_30h.

The amounts of urea can be discussed using the surface excess value reported for the urea adsorbed at the electrode/electrolyte interface, 4.96×10^{-6} mol m^{-2}.[47] Since the surface areas of TiO_2 NPs without urea are not available, we utilize the surface areas of the TiO_2 NPs with urea, 231–281 m^2 g^{-1}. The maximal values of urea for 1 g of the TiO_2 NPs can thus be estimated to be 0.0688–0.0837 g. The values listed in Table 1, on the contrary, correspond to 0.080–0.202 g of urea for 1 g of unmodified TiO_2 NPs. Thus, it is likely that large portions of the TiO_2 NP surfaces are covered with urea, and excess urea may be present in TiO_2_30h, in particular.

The amounts of Cl^- were measured by IC analysis. The amounts of Cl^- in TiO_2_30h, TiO_2_42h and TiO_2_70h were all below the limit of detection, indicating that no Ti–Cl bonds remained after the reaction for 30 h. On the other hand, the presence of Cl_2 gas was investigated with a gas detection tube. The amount of Cl_2 evolved upon opening the autoclave in a glovebag was 2.50 ppm for TiO_2_30h.

Photocatalytic activity of the TiO_2 nanoparticles dispersed in water

TiO_2_30h and TiO_2_42h were readily dispersed in water without ultrasonic treatment (Fig. S5, ESI†). The aqueous TiO_2 NP dispersions were clear and colourless. This excellent dispersibility of the TiO_2 NPs is likely to originate from the presence of hydrophilic urea on the surface. On the contrary, TiO_2_70h was not dispersed in water, probably because of its larger aggregation size.

The UV-Vis spectra of the dispersions were measured to estimate the energy band gap (E_g) (Fig. S6, ESI†). Absorptions below ~400 nm are present, and the E_g values can be estimated by the Kubelka–Munk function.[48] The estimated E_g values of TiO_2_30h and TiO_2_42h are 3.33 and 3.31 eV, respectively. These E_g values are almost equal to or slightly larger than that of pure anatase (E_g = 3.30 eV).[2]

Fig. 6 shows the photocatalytic degradation behaviour of methylene blue over TiO_2_30h and TiO_2_42h. The absorbance at 664.5 nm, assignable to methylene blue, decreases gradually under UV light irradiation. It is clearly shown that TiO_2_42h exhibits better photocatalytic activity. A possible reason for the higher photocatalytic activity of TiO_2_42h is its lower urea content.

Control experiments: preparation of the TiO_2 nanoparticles without using UHP

TiO_2_H_2O_2_urea was a mixture of a yellow liquid and white solid. TiO_2_water_urea was a mixture of a pale yellow liquid and while solid. TiO_2_H_2O_2 was a mixture of a transparent liquid and while solid. White powders were obtained after these products were washed and dried. The Ti-based yields of TiO_2_H_2O_2_urea, TiO_2_water_urea and TiO_2_H_2O_2 were 34, 23, and 63%, respectively.

Fig. 2 shows the XRD patterns of the control experiment products. TiO_2_H_2O_2_urea and TiO_2_water_urea consist of rutile TiO_2 (JCPDS no. 21-1276) and NH_4Cl (JCPDS no. 7-8). The XRD pattern of TiO_2_H_2O_2 corresponds to rutile TiO_2. The crystallite sizes of TiO_2_H_2O_2_urea, TiO_2_water_urea and TiO_2_H_2O_2 are calculated from the (110) reflections using Scherrer's formula[33] as 11, 11, 12 nm, respectively.

The control experiment products were further characterized by Raman spectroscopy (Fig. 3). The Raman spectrum of TiO_2_H_2O_2_urea shows bands at 148.3, 241.4, 437.6, and 604.7 cm^{-1}. Bands are present at 141.7, 243.0, 437.6, and 604.3 cm^{-1} in the Raman spectrum of TiO_2_water_urea. The Raman spectrum of TiO_2_H_2O_2 shows bands at 151.5, 236.6, 439.1, and 612.1 cm^{-1}. These bands are consistent with the

Table 1 The amounts of urea and water estimated by TG, ICP and IC results

Product name	Amount of urea/mass%	Amount of water/mass%
TiO_2_30h	15.5	8.0
TiO_2_42h	6.6	10.4
TiO2_70h	9.8	9.1

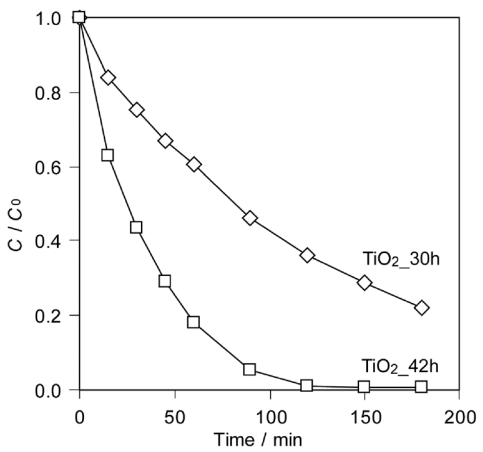

Fig. 6 Photocatalytic degradation of methylene blue by TiO_2_30h and TiO_2_42h under UV irradiation.

bands observed for rutile TiO_2,[48,49] consistent with the XRD observation.

Fig. 4 shows the IR spectra of the control experiment products. A triply degenerate bending band of NH_4^+ is present at around 1400 cm^{-1} [50] in the spectra of TiO_2_H_2O_2_urea and TiO_2_water_urea. This result suggests that NH_4^+ ions of NH_4Cl were present in TiO_2_H_2O_2_urea and TiO_2_water_urea. Thus, the IR spectral results are in accordance with the XRD observation.

Fig. 5 shows the TEM images of TiO_2_H_2O_2_urea, TiO_2_water_urea and TiO_2_H_2O_2. The control experiment products were not dispersed in water, partly because larger aggregates were present. TiO_2_H_2O_2_urea shows the presence of connected spherical TiO_2 with sizes between 200–300 nm. TiO_2_water_urea consists of undulating spherical aggregates with sizes between 100–200 nm. TiO_2_H_2O_2 is composed of the rod-like TiO_2 form echinoid-like aggregates with sizes of about 400 nm.

The presence of Cl_2 gas in the autoclaves was studied with a gas detection tube. The amount of Cl_2 in the products of TiO_2_H_2O_2_urea was below the limit of detection, 0.1 ppm.

These results clearly demonstrate that the control experiments gave rutile TiO_2, different from the synthesis using UHP, which gave anatase TiO_2. Thus, it is likely that the reaction paths for the control experiments are different from those for the synthesis using UHP. The formation conditions for rutile and anatase TiO_2 in aqueous media can be discussed based on their structural characteristics. It is widely accepted that rutile TiO_2 forms preferentially under acidic conditions in which the number of OH^- is low. Such acidic conditions are advantageous for the corner-sharing bonding of TiO_6 octahedra, leading to the formation of rutile TiO_2.[48,51] Anatase TiO_2 is preferentially formed under basic conditions, on the other hand, since the presence of a large number of OH^- increases the probability of edge-shared bonding and promotes the formation of anatase TiO_2.[48,51] In the control experiments conducted without the use of UHP, the system should consist of two immiscible phases, an aqueous phase and a CH_2Cl_2 phase. Thus, $TiCl_4$ is likely to be hydrolyzed at their interface, leading to the formation of a highly acidic aqueous phase *via* the formation of HCl. (Note that urea and ammonia, which is a hydrolysis product of urea, are weak bases, and the Cl : N molar ratio was 1 : 1.) Thus, TiO_2 should be formed under acidic conditions to generate rutile TiO_2. (The addition of urea in the preparation of TiO_2 from a $TiCl_4$ aqueous solution promoted the crystallization of anatase TiO_2, but strongly acidic aqueous phases in the control experiments seem to cause rutile TiO_2 formation.)[52] In the synthesis conducted using UHP, on the contrary, the reaction starts in a homogeneous system. It is likely that UHP directly oxidizes $TiCl_4$ in the early stage of the process, leading to the formation of anatase TiO_2. The direct reaction between $TiCl_4$ and UHP is consistent with the evolution of Cl_2 only in the synthesis with UHP, since the Cl_2 evolution indicates the presence of a redox reaction. This also indicates that, even in the presence of H_2O_2, the reactions proceed mostly *via* hydrolysis in the control experiments.

Another characteristic of the TiO_2 NPs obtained by the synthesis conducted using UHP is high dispersibility in water, a result contrary to the control experiments results. This may be ascribable to the effective adsorption of urea on the surface. Urea could be released in CH_2Cl_2, and stabilized by coordinating to the Lewis acid site on the TiO_2 NPs.

Based on the results, the reaction mechanisms of TiO_2 formation are proposed, as shown in Fig. 7. In the UHP system, $TiCl_4$ is likely to be oxidized directly by UHP to form anatase TiO_2 in the early stage of the process. Released urea molecules appear to be adsorbed on the surface of the generated TiO_2, leading to the formation of spheroid anatase TiO_2 NPs. Since HCl is likely to form during this procedure (as suggested by the formation of NH_4Cl), hydrolysis seems be involved in the latter stage. In the control reaction experiments, on the contrary, TiO_2 seems to be formed mostly *via* hydrolysis and rutile TiO_2 is formed in highly acidic aqueous media. (Note that hydrogen peroxide is available only in aqueous solutions.)

Since variations in crystallite size are not evident after 30 h, the formation of anatase TiO_2 NPs is essentially completed by 30 h. The main difference between TiO_2_30h and TiO_2_42h is the amount of adsorbed urea, possibly due to hydrolysis *via* contact with water, released from UHP. A comparison of TiO_2_30h and TiO_2_42h shows a tendency towards aggregation, and TiO_2_70h exhibits clear aggregation of the TiO_2 NPs. Since the addition of NH_4Cl promoted the aggregation of TiO_2 NPs,[53] we assume that the formation of a large amount of NH_4Cl (as shown in Fig. S1, ESI†) causes the aggregation of TiO_2 NPs in TiO_2_70h.

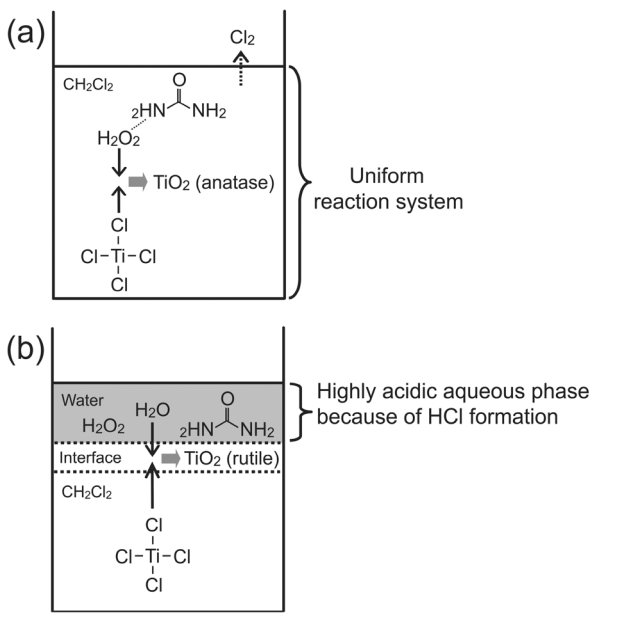

Fig. 7 Proposed mechanism of the preparation of TiO_2, (a) the $TiCl_4$–UHP–CH_2Cl_2 system (in the early stage) and (b) the control experiments.

Conclusions

Spheroid anatase TiO_2 NPs have been successfully prepared from $TiCl_4$ using urea hydrogen peroxide (UHP) as an oxygen donor through a reaction at 80 °C for 30–70 h. The anatase TiO_2 NPs exhibited high dispersibility in water, probably due to the presence of urea. The formation of Cl_2 as well as a comparison with the results of control experiments performed without UHP suggests that anatase TiO_2 NPs were formed *via* direct oxidation by UHP. The photocatalytic activity of the water-dispersible products (the reaction periods were 30 and 42 h) was estimated, and the product with a lower urea content exhibited better photocatalytic activity. The present results indicate that UHP can be utilized as an oxygen donor in preparations of TiO_2 NPs, and its use could be extended to preparations of various metal oxides.

Acknowledgements

This work was financially supported in part by a Grant-in-Aid for Scientific Research on Innovative Areas "New Polymeric Materials Based on Element-Blocks (No. 2401)" (24102002) and the Global COE program "Center for Practical Chemical Wisdom" of the Ministry of Education, Culture, Sports, Science, and Technology, Japan. The authors thank Mr. Satoru Sato for his experimental assistance.

Notes and references

1 G. A. Ozin and A. C. Arsenault, *Nanochemistry – A Chemical Approach to Nanomaterials*, RSC Publishing, London, 2006.
2 D. P. Macwan, P. N. Dave and S. Chaturvedi, *J. Mater. Sci.*, 2011, **46**, 3669–3686.
3 B. L. Cushing, V. L. Kolesnichenko and C. J. O'Connor, *Chem. Rev.*, 2004, **104**, 3893–3946.
4 J. A. Chang, M. Vithal, I. C. Baek and S. I. Seok, *J. Solid State Chem.*, 2009, **182**, 749–756.
5 D. A. H. Hanaor and C. C. Sorrell, *J. Mater. Sci.*, 2011, **46**, 855–874.
6 X. Chen and S. S. Mao, *Chem. Rev.*, 2007, **107**, 2891–2959.
7 S. M. Gupta and M. Tripathi, *Cent. Eur. J. Chem.*, 2012, **10**, 279–294.
8 Z. R. Ismagilov, L. T. Tsikoza, N. V. Shikina, V. F. Zarytova, V. V. Zinoviev and S. N. Zagrebelnyi, *Russ. Chem. Rev.*, 2009, **78**, 873–885.
9 M. Niederberger and G. Garnweitner, *Chem.–Eur. J.*, 2006, **12**, 7282–7302.
10 J. N. Hay and H. M. Raval, *Chem. Mater.*, 2001, **13**, 3396–3403.
11 P. H. Mutin and A. Vioux, *Chem. Mater.*, 2009, **21**, 582–596.
12 A. Vioux, *Chem. Mater.*, 1997, **9**, 2292–2299.
13 P. Arnal, R. J. P. Corriu, D. Leclercq, P. H. Mutin and A. Vioux, *Chem. Mater.*, 1997, **9**, 694–698.
14 A. Aboulaich, B. Boury and P. H. Mutin, *Chem. Mater.*, 2010, **22**, 4519–4521.
15 L. Y. Yang, G. P. Feng and T. X. Wang, *Mater. Lett.*, 2010, **64**, 1647–1649.
16 R. S. Sapieszko and E. Matijević, *J. Colloid Interface Sci.*, 1980, **74**, 405–422.
17 Z. Ji, S. Zhao, C. Wang and K. Liu, *Mater. Sci. Eng., B*, 2005, **117**, 63–66.
18 D. Wang, Z. Ma, S. Dai, J. Liu, Z. Nie, M. H. Engelhard, Q. Huo, C. Wang and R. Kou, *J. Phys. Chem. C*, 2008, **112**, 13499–13509.
19 M. Kakihana, M. Kobayashi, K. Tomita and V. Petrykin, *Bull. Chem. Soc. Jpn.*, 2010, **83**, 1285–1308.
20 Y. Qian, Q. Chen, Z. Chen, C. Fan and G. Zhou, *J. Mater. Chem.*, 1993, **3**, 203–205.
21 H. Ichinose, M. Terasaki and H. Katsuki, *J. Ceram. Soc. Jpn.*, 1996, **104**, 715–718.
22 H. Ichinose, M. Terasaki and H. Katsuki, *J. Sol-Gel Sci. Technol.*, 2001, **22**, 33–40.
23 N. Sasirekha, B. Rajesh and Y. W. Chen, *Thin Solid Films*, 2009, **518**, 43–48.
24 M. S. Cooper, H. Heaney, A. J. Newbold and W. R. Sanderson, *Synlett*, 1990, 533–535.
25 C. L. Fan, W.-D. Lee, N.-W. Teng, Y.-C. Sun and K. Chen, *J. Org. Chem.*, 2003, **68**, 9816–9818.
26 M. Marigo, J. Franzén, T. B. Poulsen, W. Zhuang and K. A. Jørgensen, *J. Am. Chem. Soc.*, 2005, **127**, 6964–6965.
27 M. C. Ball and S. Massey, *Thermochim. Acta*, 1995, **261**, 95–106.
28 C.-S. Lu, E. W. Hughes and P. A. Giguère, *J. Am. Chem. Soc.*, 1941, **63**, 1507–1513.
29 S. Taliansky, *Synlett*, 2005, 1962–1963.
30 A. Hasaninejad, G. Chehardoli, M. A. Zolfigol and A. Abdoli, *Phosphorus, Sulfur Silicon Relat. Elem.*, 2011, **186**, 271–280.
31 A. M. Bernhard, D. Peitz, M. Elsener, A. Wokaun and O. Kröcher, *Appl. Catal., B*, 2012, **115**, 129–137.
32 C. Wang, C. Shao, Y. Liu and X. Li, *Inorg. Chem.*, 2009, **48**, 1105–1113.
33 K. Del Ángel-Sánchez, O. Vázquez-Cuchillo, M. Salazar-Villanueva, J. F. Sánchez-Ramirez, A. Cruz-López and A. Aguilar-Elguezabal, *J. Sol-Gel Sci. Technol.*, 2011, **58**, 360–365.
34 V. Swamy, A. Kuznetsov, L. S. Dubrovinsky, R. A. Caruso, D. G. Shchukin and B. C. Muddle, *Phys. Rev. B: Condens. Matter Mater. Phys.*, 2005, **71**, 184302.
35 S. Kelly, F. H. Pollak and M. Tomkiewicz, *J. Phys. Chem. B*, 1997, **101**, 2730–2734.
36 J. C. Parker and R. W. Siegel, *J. Mater. Res.*, 1990, **5**, 1246–1252.
37 J. C. Parker and R. W. Siegel, *Appl. Phys. Lett.*, 1990, **57**, 943–945.
38 M.-H. Lee and B.-C. Choi, *J. Am. Ceram. Soc.*, 1991, **74**, 2309–2311.
39 W. Ma, Z. Lu and M. Zhang, *Appl. Phys. A: Mater. Sci. Process.*, 1998, **66**, 621–627.
40 T. Busani and R. A. B. Devine, *Semicond. Sci. Technol.*, 2005, **20**, 870–875.
41 J.-G. Li, X. Yang and T. Ishigaki, *J. Phys. Chem. B*, 2006, **110**, 14611–14618.

42 X. Xiang, L. Guo, X. Wu, X. Ma and Y. Xia, *Environ. Chem. Lett.*, 2012, **10**, 295–300.
43 M. A. Larrubia, G. Ramis and G. Busca, *Appl. Catal., B*, 2000, **27**, L145–L151.
44 A. M. Bernhard, I. Czekaj, M. Elsener and O. Kröcher, *Appl. Catal., B*, 2013, **134–135**, 316–323.
45 T. Sugimoto, X. Zhou and A. Muramatsu, *J. Colloid Interface Sci.*, 2003, **259**, 53–61.
46 K. Kanie and T. Sugimoto, *Chem. Commun.*, 2004, 1584–1585.
47 F. M. Kimmerle and H. Ménard, *Can. J. Chem.*, 1977, **55**, 3312–3320.
48 X. Shen, J. Zhang and B. Tian, *J. Hazard. Mater.*, 2011, **192**, 651–657.
49 G. A. Samara and P. S. Peercy, *Phys. Rev. B: Solid State*, 1973, **7**, 1131–1148.
50 N. E. Schumaker and C. W. Garland, *J. Chem. Phys.*, 1970, **53**, 392–407.
51 L. Kong, I. Karatchevtseva, M. Blackford, I. Chironi and G. Triani, *J. Am. Ceram. Soc.*, 2012, **95**, 816–822.
52 K. Ooi, Y. Miyai, S. Katoh and K. Sugasaka, *Bull. Chem. Soc. Jpn.*, 1988, **61**, 2721–2726.
53 W.-Y. Cheng, J. R. Deka, Y.-C. Chiang, A. Rogeau and S.-Y. Lu, *Chem. Mater.*, 2012, **24**, 3255–3262.

